Compound distributions motivated
by linear failure rate

Narjes Gitifar[1], Sadegh Rezaei[1] and Saralees Nadarajah[2]

Abstract

Motivated by three failure data sets (lifetime of patients, failure time of hard drives and failure time of a product), we introduce three different three-parameter distributions, study basic mathematical properties, address estimation by the method of maximum likelihood and investigate finite sample performance of the estimators. We show that one of the new distributions provides a better fit to each data set than eight other distributions each having three parameters and three distributions each having two parameters.

1. Introduction

Systems or components having linear failure rates are common in real life. Examples include concrete under multiaxial states of stress (Donida and Mentrasti, 1982), composite laminates with transverse shear (Reddy and Reddy, 1992) and load-sharing systems (Sutar and Naik-Nimbalkar, 2014). There are also many real data sets that exhibit approximately linear failure rates at least in the upper tails. We present three examples.

The first data set, due to Dispenzieri et al. (2012), consists of the number of days from visit to clinic until death of 100 patients. The data result from a study of the relationship between serum free light chain and mortality. The 100 patients were selected randomly from a total of 7874 patients, including patients who had not died. The patients who had died were diagnosed with monoclonal gammapothy.

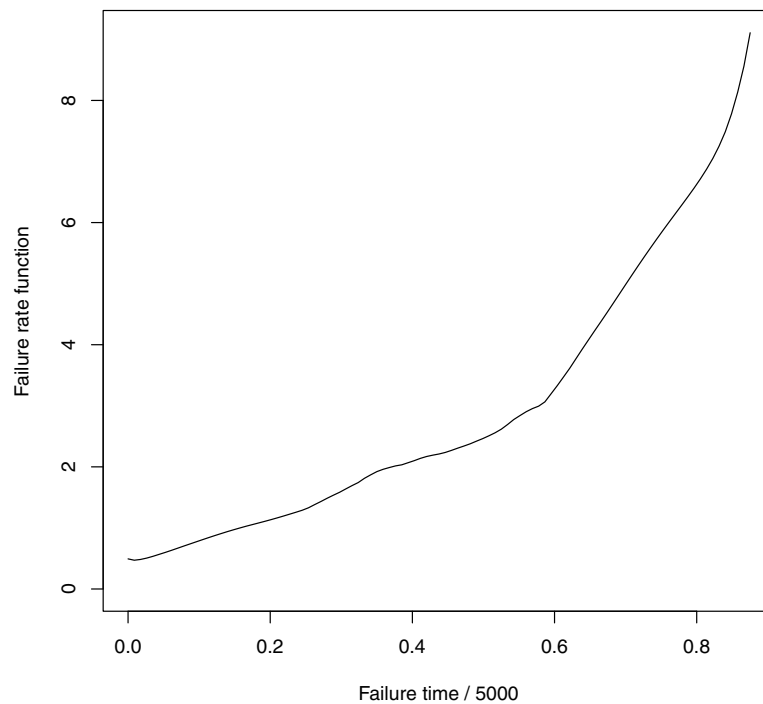[1] Amirkabir University of Technology, Tehran, IRAN, email: srezaei@aut.ac.ir

[2] University of Manchester, Manchester M13 9PL, UK

Table 1: *Summary statistics of the three data sets.*

Statistic	Data set 1	Data set 2	Data set 3
minimum	0.0054	0.0053	0.0035
first quartile	0.3368	0.3977	0.318
median	0.4774	0.7770	0.4211
third quartile	0.7412	0.9304	0.5581
maximum	0.9514	1.4040	0.6878

Figure 1: *Kaplan-Meier estimate of the failure rate function of the patient data of Dispenzieri et al. (2012).*

The second data set from https://www.backblaze.com/hard-drive-test-data.html is one hundred failure times in days of hard drives. The data were selected randomly from a total of 52422 hard drives, which included hard drives which had not failed. The data were collected by a large backup storage provider over two years. On each day, the Self-Monitoring, Analysis, and Reporting Technology (SMART) statistics of operational drives were recorded. When a hard drive was no longer operational, it was marked as a failure and removed.

The third data set due to Hong and Meeker (2013) is one hundred failure data in weeks of a product called Product D2 that is used in offices or residences. Product D2 is "similar to a high-end copying machine connected to the Internet and installed with a
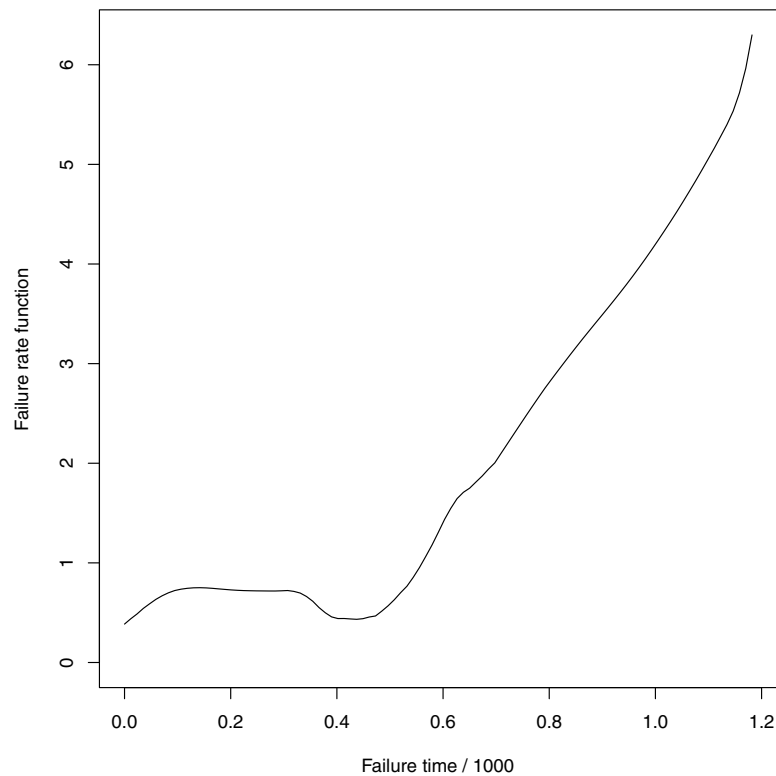
Figure 2: *Kaplan-Meier estimate of the failure rate function of the hard drive failure data.*

smart chip to record the number of pages that have been printed, as a function of time"
(Hong and Meeker, 2013, page 136). The one hundred data were selected randomly
from a total of 1800 observations.

All three data sets are presented in the appendix.

Kaplan-Meier estimates of the failure rate function (FRF) of the three data sets are
shown in Figures 1, 2 and 3. We can see that the FRFs are approximately linear at least
in the upper tails. The histogram of the three data sets are shown in Figures 8, 9 and 10.
Some summary statistics of the three data sets are shown in Table 1.

We suppose that the patient's body or the hard drive or the product D2 is made of a
number of components say *N* working independently in series. The assumption of the
series structure is more reasonable than a parallel structure because it is unlikely that
a patient's body will fail if and only if all its components fail or that a hard drive will
break if and only if all its components break or that a product will fail if and only if all
its components fail. It is more likely that a patient's body will fail if and only if any of
its components fails or that a hard drive will break if and only if any of its components
breaks or that a product will fail if and only if any of its components fails. However,
in practice the components may not work independently. The distribution of the failure
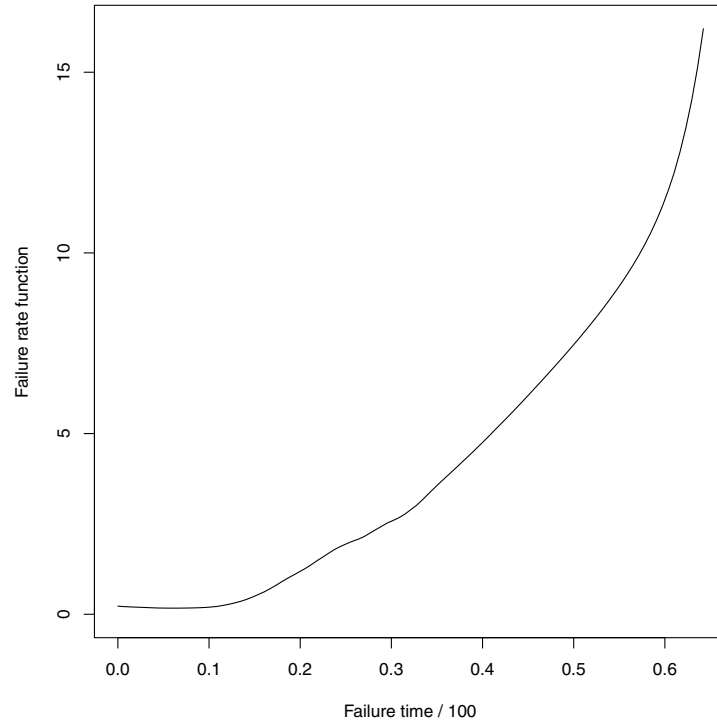
Figure 3: *Kaplan-Meier estimate of the failure rate function of the failure data of Hong and Meeker (2013).*

time may not have a closed form if we assume that the components are dependent, see (2) below and its discussion. We shall suppose independence for simplicity.

The number N may vary from one patient to another or one hard drive to another or one product to another. It may depend on the type of hard drive, type of patient, type of product, weight, length, and so on. So, we may take N as a random variable. The failure time can be written as $X = \min(Y_1, Y_2, \ldots, Y_N)$, where $Y_1, Y_2, \ldots, Y_N$ denote the failure times of the N components.

Standard models for N are the geometric, zero truncated Poisson, logarithmic, zero truncated negative binomial and zero truncated binomial distributions. For simplicity, we shall consider only the first three since each of them has one parameter. The last two distributions have two parameters each. That is, we take N to have one of the following probability mass functions (PMFs):

$$\Pr(N=n) = (1-\lambda)\lambda^{n-1}$$

for $0 < \lambda < 1$ and $n = 1, 2, \ldots$;

$$\Pr(N=n) = \frac{\lambda^n}{(e^\lambda - 1)n!}$$

for $\lambda > 0$ and $n = 1, 2, \ldots$; or

$$\Pr(N = n) = -\frac{1}{\ln(1-\lambda)} \frac{\lambda^n}{n}$$

for $0 < \lambda < 1$ and $n = 1, 2, \ldots$.

Since the failure rate for the three data sets is approximately linear at least in the upper tail (see Figures 1, 2 and 3), we shall suppose $Y_1, Y_2, \ldots$ too follow a distribution that has a linear FRF. The distribution characterized by a linear failure rate is actually known as the linear failure rate (LFR) distribution due to Bain (1974). Its probability density function (PDF) and cumulative distribution function (CDF) are specified by

$$f_Y(y; \gamma, \beta) = (\beta + \gamma y) \exp\left(-\beta y - \frac{\gamma}{2} y^2\right)$$

and

$$F_Y(y; \gamma, \beta) = 1 - \exp\left(-\beta y - \frac{\gamma}{2} y^2\right),$$

respectively, for $y > 0$, $\beta \geq 0$, $\gamma \geq 0$ and $\beta + \gamma > 0$. It is easy to see that the FRF is $h_Y(y; \gamma, \beta) = \beta + \gamma y$, a linear function of y. Both parameters, β and γ, are referred to as scale parameters.

The distribution of $X = \min(Y_1, Y_2, \ldots, Y_N)$ can now be derived given the assumptions that N is either geometric, Poisson or logarithmic and $Y_1, Y_2, \ldots$ are independent LFR random variables independent of N. In the general case, the CDF and the PDF of X can be derived as

$$F_X(x) = \Pr[\min(Y_1, Y_2, \ldots, Y_N) < x] = 1 - \Pr[\min(Y_1, Y_2, \ldots, Y_N) > x]$$

$$= 1 - \sum_{n=1}^{\infty} \Pr[\min(Y_1, Y_2, \ldots, Y_n) > x \mid N = n] \Pr(N = n)$$

$$= 1 - \sum_{n=1}^{\infty} \Pr[Y_1 > x, Y_2 > x, \ldots, Y_n > x] \Pr(N = n)$$

$$= 1 - \sum_{n=1}^{\infty} \Pr^n[Y > x] \Pr(N = n) = 1 - \sum_{n=1}^{\infty} [1 - F_Y(x)]^n \Pr(N = n)$$

and

$$f_X(x) = f_Y(x) \sum_{n=1}^{\infty} n [1 - F_Y(x)]^{n-1} \Pr(N = n),$$

respectively. In the case N is geometric, we obtain

$$f_X(x; \lambda, \gamma, \beta) = \frac{(1 - \lambda)(\beta + \gamma x) \exp\left(-\beta x - \frac{\gamma}{2} x^2\right)}{\left[1 - \lambda \exp\left(-\beta x - \frac{\gamma}{2} x^2\right)\right]^2},$$

which we shall refer to as the linear failure rate geometric (LFRG) distribution and write $X \sim \mathrm{LFRG}(\lambda, \gamma, \beta)$ for $0 < \lambda < 1$, $\beta \geq 0$, $\gamma \geq 0$ and $\beta + \gamma > 0$. In the case N is zero truncated Poisson, we obtain

$$f_X(x; \lambda, \gamma, \beta) = \lambda \left(1 - e^{-\lambda}\right)^{-1} (\beta + \gamma x) \exp\left(-\lambda - \beta x - \frac{\gamma}{2} x^2\right) \exp\left[\lambda \exp\left(-\beta x - \frac{\gamma}{2} x^2\right)\right],$$
(1)

which we shall refer to as the linear failure rate Poisson (LFRP) distribution and write $X \sim \mathrm{LFRP}(\lambda, \gamma, \beta)$ for $\lambda > 0$, $\beta \geq 0$, $\gamma \geq 0$ and $\beta + \gamma > 0$. In the case N is logarithmic, we obtain

$$f_X(x; \lambda, \gamma, \beta) = -\frac{\lambda(\beta + \gamma x) \exp\left(-\beta x - \frac{\gamma}{2} x^2\right)}{\ln(1 - \lambda)\left[1 - \lambda \exp\left(-\beta x - \frac{\gamma}{2} x^2\right)\right]},$$

which we shall refer to as the linear failure rate logarithmic (LFRL) distribution and write $X \sim \mathrm{LFRL}(\lambda, \gamma, \beta)$ for $0 < \lambda < 1$, $\beta \geq 0$, $\gamma \geq 0$ and $\beta + \gamma > 0$. These distributions do not have linear failure rates. But $h_X(y; \lambda, \gamma, \beta) \sim h_Y(y; \gamma, \beta) \sim \gamma y$ as $y \to \infty$. So, the assumption of linear failure rate for $Y_1, Y_2, \ldots$ guarantees that linear failure rate holds for X too at least in the upper tail.

The limiting cases of the LFRG, LFRP and LFRL distributions as $\lambda \downarrow 0$ is the LFR distribution. The LFRG and LFRL distributions limit to a degenerate distribution as $\lambda \uparrow 1$.

If $Y_1, Y_2, \ldots$ are dependent random variables then the CDF of X can only be expressed as

$$F_X(x) = 1 - \sum_{n=1}^{\infty} \Pr[Y_1 > x, Y_2 > x, \ldots, Y_n > x] \Pr(N = n). \qquad (2)$$

This cannot be reduced to a closed form unless the joint dependence of $(Y_1, Y_2, \ldots, Y_n)$ takes a very simple form.

In the rest of this section, Section 2 and Section 3, we shall focus on the LFRP distribution. The details for the LRFG and LRFL distributions can be derived similarly. One of the most popular models for counts is the zero truncated Poisson distribution. Some of its recent applications can be found in van der Heijden et al. (2003), Elhai et al. (2008), Ginebra and Puig (2010) and Xu and Hu (2011).
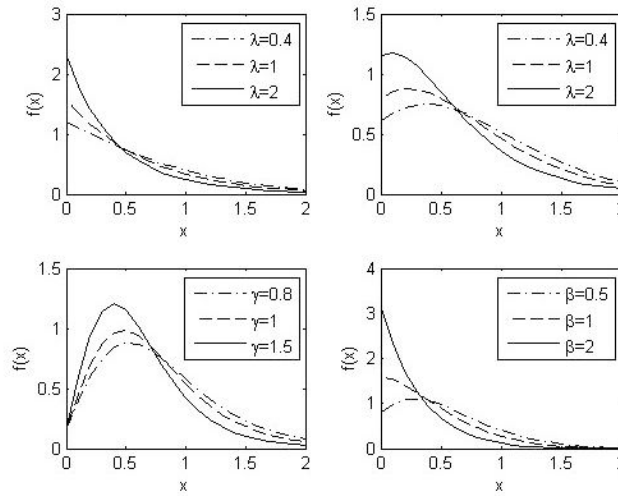
Figure 4: *Probability density function of the LFRP distribution for (a) $\gamma = 0.5$ and $\beta = 1$,*
(b) $\gamma = 1$ and $\beta = 0.5$, (c) $\beta = 0.05$ and $\lambda = 3$, (d) $\gamma = 2$ and $\lambda = 1$.

Possible shapes of (1) are shown in Figure 4. We see that both monotonically decreasing and unimodal shapes are possible. The mode of (1) is the root of

$$\frac{\gamma}{\beta + \gamma x} - \beta - \gamma x = \lambda(\beta + \gamma x)\exp\left(-\beta x - \frac{\gamma}{2}x^2\right).$$

Furthermore, $f_X(0) = \lambda\beta / \left(1 - e^{-\lambda}\right)$ and

$$f_X(x) \sim \lambda\gamma \left(1 - e^{-\lambda}\right)^{-1} x\exp\left(-\lambda - \beta x - \frac{\gamma}{2}x^2\right)$$

as $x \to \infty$. The lower tail of the PDF has a fixed point while its upper tail decays exponentially.

The CDF and FRF of $X \sim \mathrm{LFRP}(\lambda, \gamma, \beta)$ are

$$F_X(x) = \frac{1}{e^\lambda - 1}\left\{e^\lambda - \exp\left[\lambda\exp\left(-\beta x - \frac{\gamma}{2}x^2\right)\right]\right\}$$

and

$$h_X(x) = \frac{(\beta + \gamma x)\lambda\exp\left(-\beta x - \dfrac{\gamma}{2}x^2\right)}{1 - \exp\left[-\lambda\exp\left(-\beta x - \dfrac{\gamma}{2}x^2\right)\right]}, \tag{3}$$
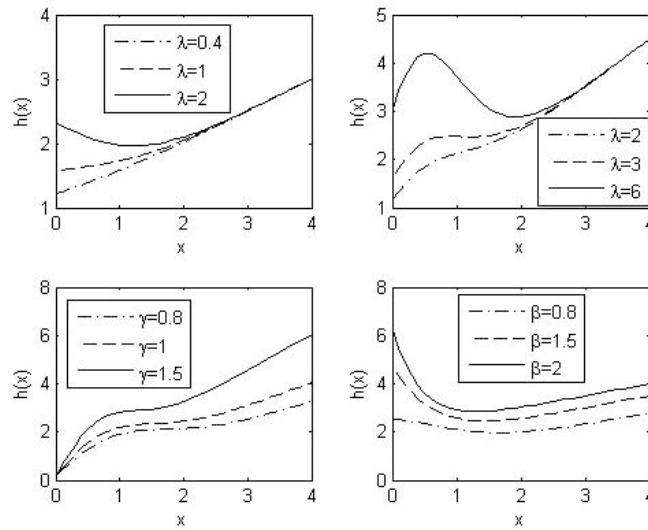
Figure 5: *Failure rate function of the LFRP distribution for (a) $\gamma = 0.5$ and $\beta = 1$,*
(b) $\gamma = 1$ and $\beta = 0.5$, (c) $\beta = 0.05$ and $\lambda = 3$, (d) $\lambda = 3$ and $\gamma = 0.5$.

respectively, for $x > 0$, $\lambda > 0$, $\beta \geq 0$, $\gamma \geq 0$ and $\beta + \gamma > 0$. Figure 5 shows possible shapes of (3) for different parameter values. We see that the LFRP distribution can exhibit increasing, decreasing and upside down bathtub shapes for the failure rate. The LFR distribution can exhibit only increasing or constant failure rates.

Reliability and survival analysis often encounter upside down bathtub failure rates. Examples can be found in redundancy allocations in systems (Singh and Misra, 1994) and mortality modelling (Silva et al., 2010).

The mode or the anti-mode of (3) is the root of

$$\frac{\gamma}{\beta + \gamma x} - \beta - \gamma x = -\lambda(\beta + \gamma x)\exp\left(-\beta x - \frac{\gamma}{2}x^2\right)\left\{\exp\left[\lambda\exp\left(-\beta x - \frac{\gamma}{2}x^2\right)\right] - 1\right\}^{-1}.$$

Furthermore, $h_X(0) = \lambda\beta/\left(1 - e^{-\lambda}\right)$ and $h_X(x) \sim \gamma x$ as $x \to \infty$. The lower tail of the FRF has a fixed point. As already noted, the upper tail of the FRF of the LFRP distribution behaves in the same manner as that of the LFR distribution. Yet the former does exhibit upside down bathtub failure rates while the latter does not.

The qth quantile of $X \sim \text{LFRP}(\lambda, \gamma, \beta)$ say x_q defined by $F_X(x_q) = q$ is

$$x_q = -\frac{\beta}{\gamma} + \sqrt{\frac{\beta^2}{\gamma^2} - \frac{2}{\gamma}\ln\left\{\ln\left[e^\lambda - q\left(e^\lambda - 1\right)\right]^{\frac{1}{\lambda}}\right\}}.$$

In particular, the median of X is

$$\text{Median}(X) = -\frac{\beta}{\gamma} + \sqrt{\frac{\beta^2}{\gamma^2} - \frac{2}{\gamma}\ln\left\{\ln\left[e^\lambda - \frac{1}{2}\left(e^\lambda - 1\right)\right]^{\frac{1}{\lambda}}\right\}}.$$

Quantiles are useful for estimation and simulation.

Several other distributions have been introduced in the literature by taking $X = \min(Y_1, Y_2, \ldots, Y_N)$, where N is a geometric, zero truncated Poisson or a logarithmic random variable: By taking N to be a geometric random variable and $Y_1, Y_2, \ldots$ to be independent and identical Weibull random variables, Barreto-Souza et al. (2011) introduced the three-parameter Weibull geometric (WG) distribution given by the PDF

$$f(x) = \frac{(1-\lambda)\beta\gamma^{-\beta}x^{\beta-1}\exp\left[-(x/\gamma)^\beta\right]}{\left\{1 - \lambda\exp\left[-(x/\gamma)^\beta\right]\right\}^2}$$

for $x > 0$, $0 < \lambda < 1$, $\beta > 0$ and $\gamma > 0$; By taking N to be a zero truncated Poisson random variable and $Y_1, Y_2, \ldots$ to be independent and identical Weibull random variables, Lu and Shi (2012) introduced the three-parameter Weibull Poisson (WP) distribution given by the PDF

$$f(x) = \frac{\lambda\beta\gamma^{-\beta}x^{\beta-1}\exp\left\{-(x/\gamma)^\beta + \lambda\exp\left[-(x/\gamma)^\beta\right]\right\}}{\exp(\lambda) - 1}$$

for $x > 0$, $\lambda > 0$, $\beta > 0$ and $\gamma > 0$; By taking N to be a logarithmic random variable and $Y_1, Y_2, \ldots$ to be independent and identical Weibull random variables, Ciumara and Preda (2009) introduced the three-parameter Weibull logarithmic (WL) distribution given by the PDF

$$f(x) = -\frac{(1-\lambda)\beta\gamma^{-\beta}x^{\beta-1}\exp\left[-(x/\gamma)^\beta\right]}{\ln\lambda\left\{1 - (1-\lambda)\exp\left[-(x/\gamma)^\beta\right]\right\}}$$

for $x > 0$, $0 < \lambda < 1$, $\beta > 0$ and $\gamma > 0$; By taking N to be a geometric random variable and $Y_1, Y_2, \ldots$ to be independent and identical generalized exponential random variables, Mahmoudi and Jafari (2012) introduced the three-parameter generalized exponential geometric (GEG) distribution given by the PDF

$$f(x) = \frac{(1-\lambda)\beta\gamma\exp(-\gamma x)\left[1 - \exp(-\gamma x)\right]^{\beta-1}}{\left\{\lambda\left[1 - \exp(-\gamma x)\right]^\beta - 1\right\}^2}$$

for $x > 0$, $0 < \lambda < 1$, $\beta > 0$ and $\gamma > 0$; By taking N to be a zero truncated Poisson random variable and $Y_1, Y_2, \ldots$ to be independent and identical generalized exponential random variables, Mahmoudi and Jafari (2012) introduced the three-parameter generalized exponential Poisson (GEP) distribution given by the PDF

$$f(x) = \frac{\lambda\beta\gamma\exp(-\gamma x)\left[1-\exp(-\gamma x)\right]^{\beta-1}\exp\left\{\left[1-\exp(-\gamma x)\right]^{\beta}\right\}}{\exp(\lambda)-1}$$

for $x > 0$, $\lambda > 0$, $\beta > 0$ and $\gamma > 0$; By taking N to be a logarithmic random variable and $Y_1, Y_2, \ldots$ to be independent and identical generalized exponential random variables, Mahmoudi and Jafari (2012) introduced the three-parameter generalized exponential logarithmic (GEL) distribution given by the PDF

$$f(x) = \frac{\lambda\beta\gamma\exp(-\gamma x)\left[1-\exp(-\gamma x)\right]^{\beta-1}}{\ln(1-\lambda)\left\{\lambda\left[1-\exp(-\gamma x)\right]^{\beta}-1\right\}}$$

for $x > 0$, $0 < \lambda < 1$, $\beta > 0$ and $\gamma > 0$.

A final motivation for the LFRP distribution is that it provides better fits for the three data sets than at least eight other distributions each having three parameters and at least three distributions each having two parameters. The eight distributions are the LFRG, LFRL, WG, WP, WL, GEG, GEP and GEL distributions.

The rest of this paper is organized as follows: estimation of the parameters of the LFRP distribution by the method of maximum likelihood is considered in Section 2; finite sample performance of the maximum likelihood estimators is assessed by simulation in Section 3; application of the LFRP distribution to the three data sets is illustrated in Section 4; some conclusions are noted in Section 5.

We have given above simple expressions for the PDF, its shape, FRF, its shape, quantiles and median of $X \sim \mathrm{LFRP}(\lambda, \gamma, \beta)$. Simple expressions for further mathematical properties of $X \sim \mathrm{LFRP}(\lambda, \gamma, \beta)$ do not appear to be possible; for example, using the series expansions

$$(1-z)^{-2} = \sum_{k=0}^{\infty}\binom{-2}{k}(-z)^{k},$$

$$\exp(z) = \sum_{k=0}^{\infty}\frac{z^{k}}{k!},$$

$$(1-z)^{-1} = \sum_{k=0}^{\infty}z^{k},$$

and equation (2.3.15.3) in Prudnikov et al. (1986), one can express the *n*th moments of LFRG, LFRP and LFRL distributions as

$$E\left(X^n\right) = (1 - \lambda) \sum_{k=0}^{\infty} \binom{-2}{k} (-\lambda)^k A(n, k),$$

$$E\left(X^n\right) = \frac{\lambda e^{-\lambda}}{1 - e^{-\lambda}} \sum_{k=0}^{\infty} \frac{\lambda^k}{k!} A(n, k)$$

and

$$E\left(X^n\right) = -\frac{1}{\ln(1 - \lambda)} \sum_{k=0}^{\infty} \lambda^{k+1} A(n, k),$$

respectively, where

$$A\left(n, k\right) = \frac{n! \exp\left[\frac{(k+1)\beta^2}{4\gamma}\right]}{\gamma^{\frac{n+1}{2}} (k+1)^{\frac{n+2}{2}}} \left[\beta \sqrt{k+1} D_{-n-1}\left(\frac{\beta \sqrt{k+1}}{\sqrt{\gamma}}\right) + (n+1) \sqrt{\gamma} D_{-n-2}\left(\frac{\beta \sqrt{k+1}}{\sqrt{\gamma}}\right)\right],$$

where $D_\nu(\cdot)$ denotes the parabolic cylinder function of order ν. These expressions are not simple. They are infinite sums of terms involving a special function which is defined in terms of an integral. So, the moments could be computed more efficiently by numerical integration, i.e., by

$$E\left(X^n\right) = \int_0^{\infty} x^n \frac{(\beta + \gamma x) \exp\left(-\beta x - \frac{\gamma}{2} x^2\right)}{\left[1 - (1 - \lambda) \exp\left(-\beta x - \frac{\gamma}{2} x^2\right)\right]^2} dx,$$

$$E\left(X^n\right) = \lambda e^{-\lambda} \left(1 - e^{-\lambda}\right)^{-1} \int_0^{\infty} x^n (\beta + \gamma x) \exp\left(-\beta x - \frac{\gamma}{2} x^2\right) \exp\left[\lambda \exp\left(-\beta x - \frac{\gamma}{2} x^2\right)\right] dx$$

and

$$E\left(X^n\right) = -\frac{1}{\ln(1 - \lambda)} \int_0^{\infty} x^n \frac{(\beta + \gamma x) \exp\left(-\beta x - \frac{\gamma}{2} x^2\right)}{1 - (1 - \lambda) \exp\left(-\beta x - \frac{\gamma}{2} x^2\right)} dx.$$

Hence, we shall not consider further mathematical properties.

2. Estimation

We suppose $x_1, x_2, \ldots, x_n$ is a random sample from $\mathrm{LFRP}(\beta, \gamma, \lambda)$ with β, γ, λ unknown. Then the log-likelihood function of β, γ, λ can be expressed as

$$\ln L = n \ln \lambda - n \ln \left(e^{\lambda} - 1 \right) + \sum_{i=1}^{n} \ln \left(\beta + \gamma x_i \right) - \beta \sum_{i=1}^{n} x_i + \frac{\gamma}{2} \sum_{i=1}^{n} x_i^2 +$$
$$+ \lambda \sum_{i=1}^{n} \exp \left(-\beta x_i - \frac{\gamma}{2} x_i^2 \right). \tag{4}$$

The associated normal equations are

$$\frac{\partial \ln L}{\partial \lambda} = \frac{n}{\lambda} - \frac{n e^{\lambda}}{e^{\lambda} - 1} + \sum_{i=1}^{n} \exp \left(-\beta x_i - \frac{\gamma}{2} x_i^2 \right),$$
$$\frac{\partial \ln L}{\partial \gamma} = \sum_{i=1}^{n} \frac{x_i}{\beta + \gamma x_i} - \frac{1}{2} \sum_{i=1}^{n} x_i^2 - \lambda \sum_{i=1}^{n} \frac{x_i^2}{2} \exp \left(-\beta x_i - \frac{\gamma}{2} x_i^2 \right),$$
$$\frac{\partial \ln L}{\partial \beta} = \sum_{i=1}^{n} \frac{1}{\beta + \gamma x_i} - \sum_{i=1}^{n} x_i + \lambda \sum_{i=1}^{n} x_i \exp \left(-\beta x_i - \frac{\gamma}{2} x_i^2 \right).$$

The maximum likelihood estimates of (λ, γ, β) say $\left(\widehat{\lambda}, \widehat{\gamma}, \widehat{\beta} \right)$ are the simultaneous solutions of $\partial \ln L / \partial \lambda = 0$, $\partial \ln L / \partial \gamma = 0$ and $\partial \ln L / \partial \beta = 0$. These equations being nonlinear, some quasi-Newton algorithm will be needed to solve them simultaneously. An alternative is to obtain $\left(\widehat{\lambda}, \widehat{\gamma}, \widehat{\beta} \right)$ by direct numerical maximization of (4). We shall pursue this simpler approach. Numerical maximization of (4) was performed by using optim in R (R Development Core Team, 2014). Extensive numerical calculations showed that the surface of (4) was reasonably smooth. optim was able to locate the maximum for a wide range of starting values. The solution returned by optim was unique for all starting values.

Reasonable starting values for the parameters are useful to ease optimization. The method of moments can be used to obtain them. Equating the sample moments $m_1 = (1/n) \sum_{i=1}^{n} x_i$, $m_2 = (1/n) \sum_{i=1}^{n} x_i^2$ and $m_3 = (1/n) \sum_{i=1}^{n} x_i^3$ with the theoretical versions given by

$$E\left(X^i \right) = \lambda \left(1 - e^{-\lambda} \right)^{-1} \int_0^{\infty} x^i (\beta + \gamma x) \exp \left(-\lambda - \beta x - \frac{\gamma}{2} x^2 \right) \exp \left[\lambda \exp \left(-\beta x - \frac{\gamma}{2} x^2 \right) \right] dx,$$

we have $m_1 = E(X)$, $m_2 = E\left(X^2 \right)$ and $m_3 = E\left(X^3 \right)$. These equations were solved using a quasi-Newton algorithm.

The distribution of $\left(\widehat{\lambda}, \widehat{\gamma}, \widehat{\beta}\right)$ as $n \to \infty$, under certain regularity conditions (see, for example, Ferguson, 1996 and pages 461-463 in Lehmann and Casella, 1998), is trivariate normal with mean (λ, β, γ) and covariance given by the inverse of

$$
\mathbf{I} = \begin{pmatrix} I_{11} & I_{12} & I_{13} \\ I_{21} & I_{22} & I_{23} \\ I_{31} & I_{32} & I_{33} \end{pmatrix} = \begin{pmatrix} \mathrm{E}\left(-\dfrac{\partial^2 \ln L}{\partial \lambda^2}\right) & \mathrm{E}\left(-\dfrac{\partial^2 \ln L}{\partial \lambda \partial \gamma}\right) & \mathrm{E}\left(-\dfrac{\partial^2 \ln L}{\partial \lambda \partial \beta}\right) \\ \mathrm{E}\left(-\dfrac{\partial^2 \ln L}{\partial \gamma \partial \lambda}\right) & \mathrm{E}\left(-\dfrac{\partial^2 \ln L}{\partial \gamma^2}\right) & \mathrm{E}\left(-\dfrac{\partial^2 \ln L}{\partial \gamma \partial \beta}\right) \\ \mathrm{E}\left(-\dfrac{\partial^2 \ln L}{\partial \beta \partial \lambda}\right) & \mathrm{E}\left(-\dfrac{\partial^2 \ln L}{\partial \beta \partial \gamma}\right) & \mathrm{E}\left(-\dfrac{\partial^2 \ln L}{\partial \beta^2}\right) \end{pmatrix}.
$$

$\mathbf{I}$ is referred to as the expected information matrix.

In practice, n is finite. Cox and Hinkley (1979) recommended that the distribution of $\left(\widehat{\lambda}, \widehat{\gamma}, \widehat{\beta}\right)$ be approximated by a trivariate normal distribution with mean (λ, β, γ) and covariance taken to be the inverse of

$$
\mathbf{J} = \begin{pmatrix} J_{11} & J_{12} & J_{13} \\ J_{21} & J_{22} & J_{23} \\ J_{31} & J_{32} & J_{33} \end{pmatrix} = \left. \begin{pmatrix} -\dfrac{\partial^2 \ln L}{\partial \lambda^2} & -\dfrac{\partial^2 \ln L}{\partial \lambda \partial \gamma} & -\dfrac{\partial^2 \ln L}{\partial \lambda \partial \beta} \\ -\dfrac{\partial^2 \ln L}{\partial \gamma \partial \lambda} & -\dfrac{\partial^2 \ln L}{\partial \gamma^2} & -\dfrac{\partial^2 \ln L}{\partial \gamma \partial \beta} \\ -\dfrac{\partial^2 \ln L}{\partial \beta \partial \lambda} & -\dfrac{\partial^2 \ln L}{\partial \beta \partial \gamma} & -\dfrac{\partial^2 \ln L}{\partial \beta^2} \end{pmatrix} \right|_{\lambda=\widehat{\lambda},\gamma=\widehat{\gamma},\beta=\widehat{\beta}}.
$$

$\mathbf{J}$ is referred to as the observed information matrix. Cox and Hinkley (1979)'s approximation is known to be a better approximation than one based on the expected information matrix.

The elements of the observed information matrix are

$$
J_{11} = \frac{n}{\widehat{\lambda}^2} - \frac{n e^{\widehat{\lambda}}}{\left(e^{\widehat{\lambda}} - 1\right)^2},
$$

$$
J_{22} = \sum_{i=1}^{n} \frac{x_i^2}{\left(\widehat{\beta} + \widehat{\gamma} x_i\right)^2} - \frac{\widehat{\lambda}}{4} \sum_{i=1}^{n} x_i^4 \exp\left(-\widehat{\beta} x_i - \frac{\widehat{\gamma}}{2} x_i^2\right),
$$

$$
J_{33} = \sum_{i=1}^{n} \frac{1}{\left(\widehat{\beta} + \widehat{\gamma} x_i\right)^2} - \widehat{\lambda} \sum_{i=1}^{n} x_i^2 \exp\left(-\widehat{\beta} x_i - \frac{\widehat{\gamma}}{2} x_i^2\right),
$$

$$
J_{12} = J_{21} = \frac{1}{2} \sum_{i=1}^{n} x_i^2 \exp\left(-\widehat{\beta} x_i - \frac{\widehat{\gamma}}{2} x_i^2\right),
$$

$$J_{13} = J_{31} = \sum_{i=1}^{n} x_i \exp\left(-\widehat{\beta} x_i - \frac{\widehat{\gamma}}{2} x_i^2\right),$$

$$J_{23} = J_{32} = \sum_{i=1}^{n} \frac{x_i}{\left(\widehat{\beta} + \widehat{\gamma} x_i\right)^2} - \frac{\widehat{\lambda}}{2} \sum_{i=1}^{n} x_i^3 \exp\left(-\widehat{\beta} x_i - \frac{\widehat{\gamma}}{2} x_i^2\right).$$

The regularity conditions referred to hold as $n \to \infty$. In practice, n is finite. So, it is natural to ask: how large n should be for the maximum likelihood estimates to perform well? We answer this question in Section 3.

3. Simulation

Here, we assess the performance of the maximum likelihood estimates with respect to sample size n. The assessment is based on a simulation study:

1. generate ten thousand samples of size n from (1). The inversion method was used to generate samples.

2. compute the maximum likelihood estimates for the ten thousand samples, say $\left(\widehat{\lambda}_i, \widehat{\beta}_i, \widehat{\gamma}_i\right)$ for $i = 1, 2, \ldots, 10000$.

3. compute the biases and mean squared errors given by

$$\text{bias}_h(n) = \frac{1}{10000} \sum_{i=1}^{10000} \left(\widehat{h}_i - h\right),$$

and

$$\text{MSE}_h(n) = \frac{1}{10000} \sum_{i=1}^{10000} \left(\widehat{h}_i - h\right)^2$$

for $h = \lambda, \beta, \gamma$.

We repeated these steps for $n = 10, 11, \ldots, 100$ with $\lambda = 1$, $\beta = 1$ and $\gamma = 1$, so computing $\text{bias}_\lambda(n)$, $\text{bias}_\beta(n)$, $\text{bias}_\gamma(n)$ and $\text{MSE}_\lambda(n)$, $\text{MSE}_\beta(n)$, $\text{MSE}_\gamma(n)$ for $n = 10, 11, \ldots, 100$.

Figures 6 and 7 show how the three biases and the three mean squared errors vary with respect to n. The broken lines in Figure 6 correspond to the biases being zero. The broken lines in Figure 7 correspond to the mean squared errors being zero. The following observations can be made:
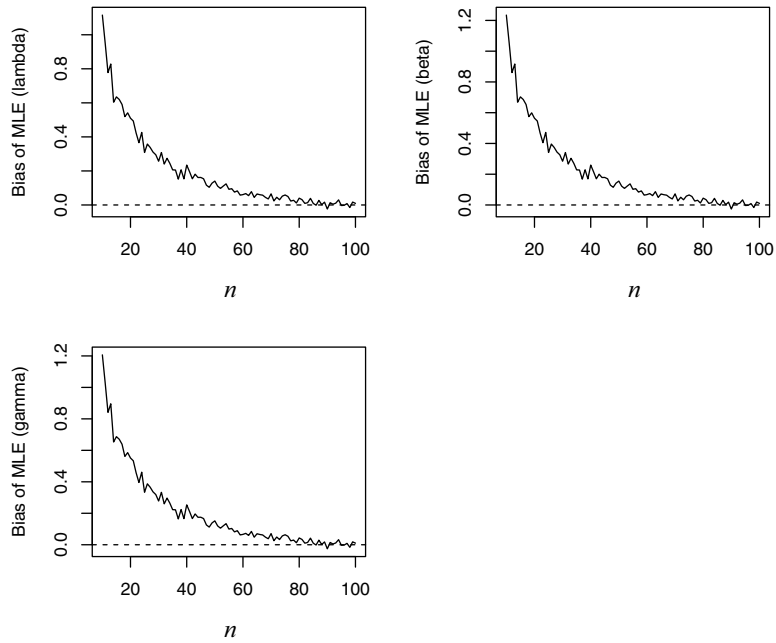
Figure 6: *From top to bottom and from left to right:*
bias$_\lambda(n)$, bias$_\beta(n)$ *and* bias$_\gamma(n)$ *versus* $n = 10, 11, \ldots, 100$.
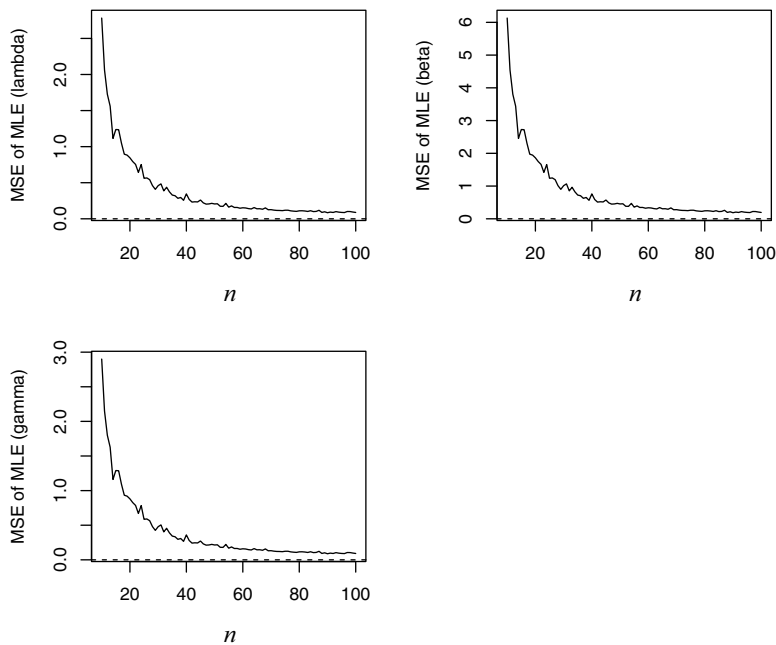

Figure 7: *From top to bottom and from left to right:*
MSE$_\lambda(n)$, MSE$_\beta(n)$ *and* MSE$_\gamma(n)$ *versus* $n = 10, 11, \ldots, 100$.

1. the biases for each parameter are generally positive;
2. the biases for each parameter decrease to zero as $n \to \infty$;
3. the biases appear smallest for the parameter, λ;
4. the mean squared errors for each parameter decrease to zero as $n \to \infty$;
5. the mean squared errors appear smallest for the parameter, λ;
6. the mean squared errors appear largest for the parameter, β;
7. the biases and mean squared errors for each parameter appear reasonably small for all $n \geq 60$.

We have presented results for only one choice for (λ, β, γ), namely that $(\lambda, \beta, \gamma) = (1, 1, 1)$. But the results were similar for a wide range of other choices. In particular, the biases and mean squared errors for each parameter appeared reasonably small for all $n \geq 60$.

The three real data sets in Section 4 each has a sample size greater than or equal to sixty. So, we can expect the estimates in Section 4 to be reasonable.

4. Real data applications

Here, we return to the three data sets to illustrate the applicability of the LFRP distribution. The following distributions were fitted to each data: the LFR, LFRG, LFRP, LFRL, WG, WP, WL, GEG, GEP and GEL distributions. We also fitted the Weibull and gamma distributions given by the PDFs

$$f(x) = \frac{\beta x^{\beta-1}}{\gamma^{\beta}} \exp\left[-\left(\frac{x}{\gamma}\right)^{\beta}\right]$$

and

$$f(x) = \frac{x^{\beta-1}}{\gamma^{\beta}\Gamma(\beta)} \exp\left(-\frac{x}{\gamma}\right),$$

respectively, for $x > 0$, $\alpha > 0$ and $\beta > 0$. Each distribution was fitted by the method of maximum likelihood. The parameter estimates, standard errors, $-\ln L$, AIC values and BIC values are given in Tables 2, 3 and 4. The standard errors were computed by inverted the observed information matrices.

We see that the LFRP distribution yields the smallest $-\ln L$, the smallest AIC and the smallest BIC for each data set. It provides a significantly better fit than the LFR distribution for each data set, as judged by the likelihood ratio test. The standard errors for the LFRP distribution appear reasonable, as they are smaller than the parameter estimates.

Table 2: *Parameter estimates, standard errors, log-likelihood, AIC and BIC for the twelve distributions fitted to the patient data of Dispenzieri et al. (2012).*

| Distribution	$\widehat{\lambda}$	SE	$\widehat{\beta}$	SE	$\widehat{\gamma}$	SE	$-\ln L$	AIC	BIC
LFR			0.348	0.176	5.071	0.739	7.747	19.494	24.704
LFRG	0.001	0.000	0.348	0.176	5.069	0.738	7.751	21.503	29.318
LFRP	1.894	0.851	1.132	0.661	5.591	1.212	4.960	15.921	23.736
LFRL	0.001	0.000	0.342	0.173	5.063	0.734	7.750	21.500	29.315
WG	0.999	0.000	1.839	0.156	0.561	0.032	11.838	29.676	37.491
WP	2.230	0.910	1.434	0.204	0.394	0.065	8.818	23.637	31.452
WL	0.001	0.000	1.848	0.157	0.563	0.032	11.841	29.682	37.498
GEG	0.999	0.000	2.012	0.285	2.925	0.307	21.182	48.365	56.180
GEP	3.850	1.032	1.095	0.326	3.947	0.377	11.689	29.377	37.193
GEL	0.001	0.000	2.011	0.285	2.923	0.307	21.184	48.368	56.183
Weibull			1.839	0.156	0.561	0.032	11.837	27.674	32.885
Gamma			2.068	0.272	0.245	0.036	19.387	42.774	47.985

Table 3: *Parameter estimates, standard errors, log-likelihood, AIC and BIC for the twelve distributions fitted to the hard drive failure data.*

Distribution	$\widehat{\lambda}$	SE	$\widehat{\beta}$	SE	$\widehat{\gamma}$	SE	$-\ln L$	AIC	BIC
LFR			0.296	0.138	2.530	0.393	42.043	88.087	93.297
LFRG	0.000	0.000	0.292	0.135	2.465	0.384	42.072	90.143	97.959
LFRP	1.753	0.691	0.776	0.375	2.841	0.572	38.849	83.698	91.514
LFRL	0.000	0.000	0.296	0.138	2.530	0.393	42.044	90.088	97.904
WG	0.999	0.000	1.751	0.152	0.774	0.046	46.993	99.986	107.801
WP	1.831	0.738	1.484	0.189	0.584	0.079	43.848	93.695	101.511
WL	0.001	0.000	1.772	0.154	0.774	0.045	46.984	99.967	107.783
GEG	0.999	0.000	1.842	0.257	2.017	0.216	55.885	117.769	125.585
GEP	3.569	1.080	1.016	0.327	2.664	0.256	47.407	100.814	108.629
GEL	0.000	0.000	1.876	0.263	2.035	0.217	55.887	117.774	125.589
Weibull			1.772	0.154	0.775	0.045	46.982	97.964	103.174
Gamma			1.902	0.249	0.369	0.055	54.304	112.608	117.818

The parameter estimates and the log-likelihood values of the LFRG and LFRL distributions are very close for all three data sets. This suggests that the likelihood surfaces for the LFRG and LFRL distributions attain their maximum points along the border corresponding to $\lambda = 0$. We noted earlier LFRG and LFRL distributions reduce to the LFR distribution as $\lambda \downarrow 0$. So, the fits of LFRG and LFRL distributions do not improve on the fit of the LFR distribution for the three data sets.

Table 4: *Parameter estimates, standard errors, log-likelihood, AIC and BIC for the twelve distributions fitted to the failure data of Hong and Meeker (2013).*

Distribution	$\widehat{\lambda}$	SE	$\widehat{\beta}$	SE	$\widehat{\gamma}$	SE	$-\ln L$	AIC	BIC
LFR			0.028	0.061	9.349	0.968	−32.148	−60.296	−55.086
LFRG	0.000	0.000	0.047	0.081	9.523	1.000	−32.069	−58.138	−50.323
LFRP	5.023	1.719	1.361	1.458	15.188	3.681	−48.555	−91.111	−83.295
LFRL	0.000	0.000	0.019	0.052	9.389	0.967	−32.133	−58.267	−50.451
WG	0.999	0.000	3.149	0.256	0.482	0.016	−44.743	−83.485	−75.670
WP	4.940	1.837	1.703	0.313	0.287	0.054	−46.938	−87.876	−80.061
WL	0.000	0.000	3.146	0.255	0.483	0.016	−44.745	−83.489	−75.674
GEG	0.003	0.000	4.552	0.476	0.753	0.133	−29.354	−52.708	−44.893
GEP	8.160	1.966	1.859	0.584	7.352	0.588	−42.532	−79.064	−71.249
GEL	2.082×10^{-5}	0.000	5.546	0.918	5.304	0.442	−25.126	−44.253	−36.437
Weibull			3.146	0.255	0.483	0.016	−44.745	−85.489	−80.279
Gamma			5.371	0.735	0.081	0.012	−31.814	−59.629	−54.418
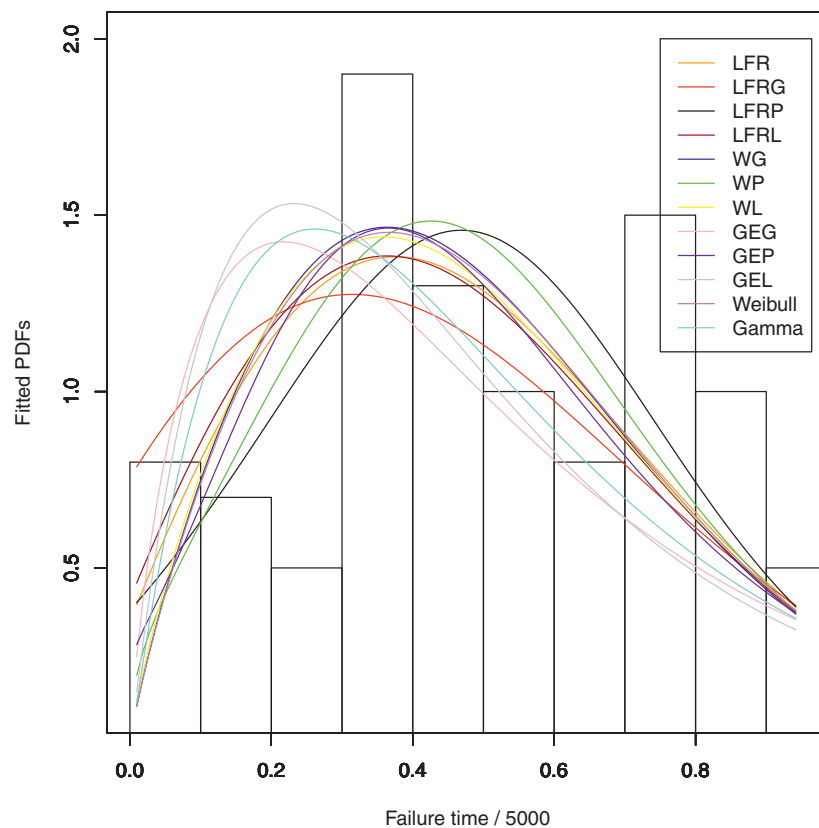
Figure 8: *Density plots for the twelve distributions fitted to the patient data of Dispenzieri et al. (2012).*
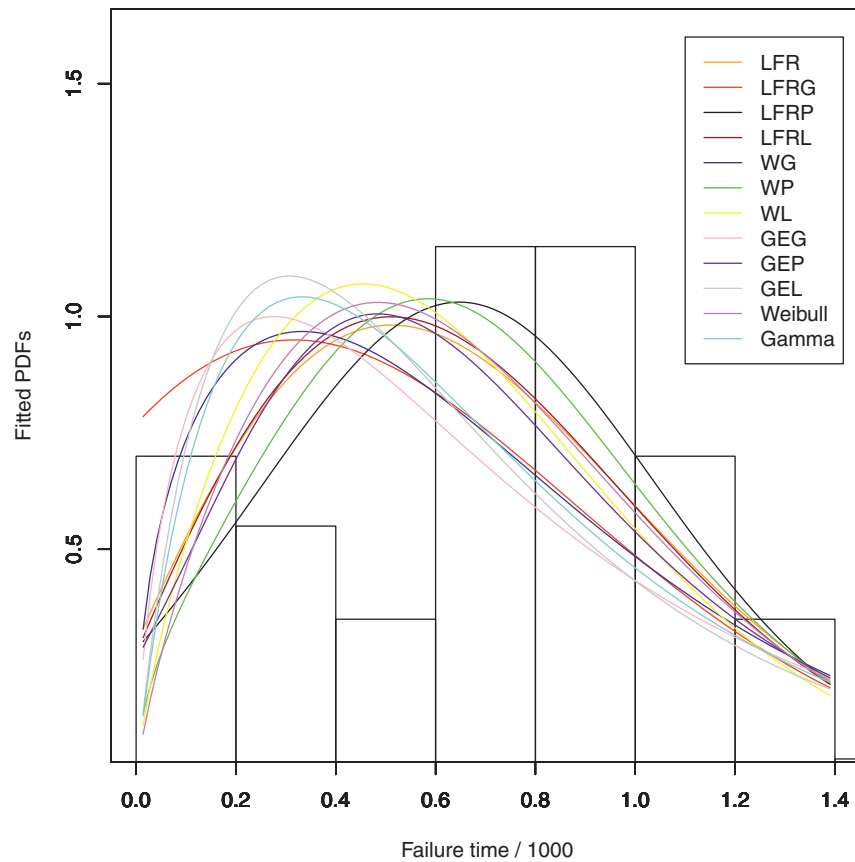
Figure 9: *Density plots for the twelve distributions fitted to the hard drive failure data.*

The density plots for the fit of the distributions for the three data sets are shown in Figures 8 to 10. The fitted PDFs of the LFRP distribution captures the observed histograms better than others. Hence, we can say that the LFRP distribution provides the best fit for at least three real data sets.

The parameter estimates of the best fitting LFRP distribution for the three data sets can be interpreted as follows:

- the patient's body can be modelled as a series system having an average of $\widehat{\lambda}/\left[1-e^{-\widehat{\lambda}}\right] = 2.2$ components with the 95 percent confidence interval $(0.37, 4.09)$, where the failure rate of each component is linear with an intercept of 1.132 and a slope of 5.591. That is, the failure rate of each component at time zero is 1.132 and the failure rate increases by 5.591 for every unit increase in time;

- the hard drive can be modelled as a series system having an average of $\widehat{\lambda}/\left[1-e^{-\widehat{\lambda}}\right] = 2.1$ components with the 95 percent confidence interval $(1.26, 2.98)$, where the failure rate of each component is linear with an intercept of 0.776 and

a slope of 2.841. That is, the failure rate of each component at time zero is 0.776 and the failure rate increases by 2.841 for every unit increase in time;

- the product D2 can be modelled as a series system having an average of $\widehat{\lambda} / \left[1 - e^{-\widehat{\lambda}} \right] = 5.1$ components with the 95 percent confidence interval $(-1.97, 12.08)$, where the failure rate of each component is linear with an intercept of 1.361 and a slope of 15.188. That is, the failure rate of each component at time zero is 1.361 and the failure rate increases by 15.188 for every unit increase in time.

Note that $\lambda / \left[1 - e^{-\lambda} \right]$ is the expected value of a zero truncated Poisson random variable. The stated confidence intervals were obtained by the delta method.
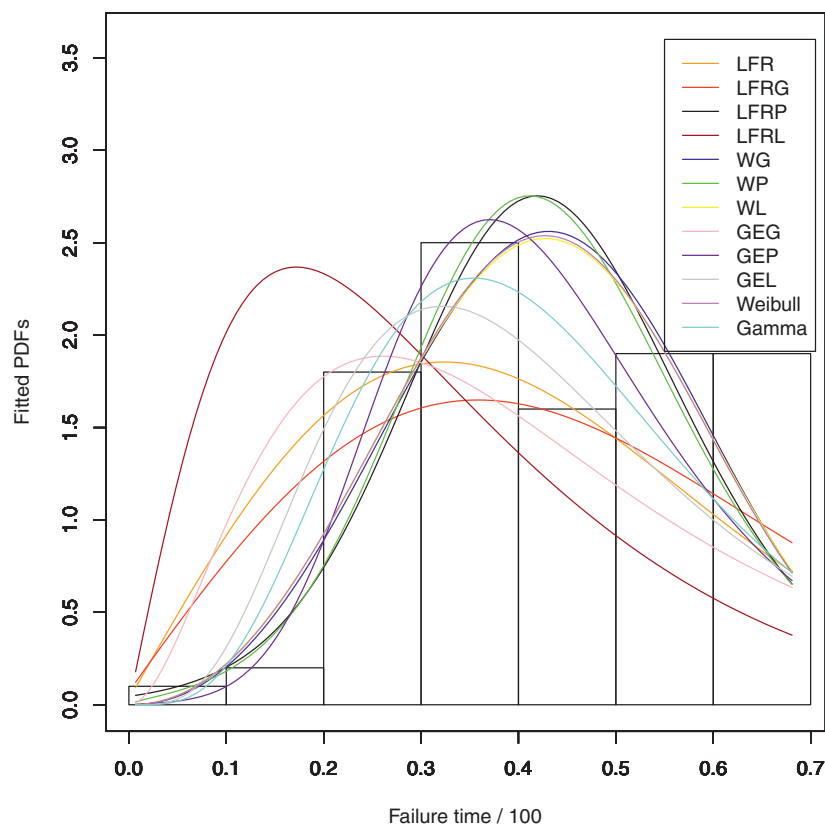

Figure 10: *Density plots for the twelve distributions fitted to the failure data of Hong and Meeker (2013).*

5. Conclusions

We have proposed three distributions motivated by three failure data sets: the linear failure rate geometric, linear failure rate Poisson and linear failure rate logarithmic distributions. Each of these distributions has three parameters.

We have studied mathematical properties and estimation issues for the linear failure rate Poisson distribution. We have shown in particular that its failure rate function can be decreasing, increasing and upside down bathtub shaped, more varied than the failure rate function of the linear failure rate distribution.

Among the twelve distributions fitted to the three data sets, the linear failure rate Poisson distribution gave the best fit. The adequacy of fits was assessed in terms AIC values, BIC values and density plots.

A future work is to estimate the parameters of the linear failure rate Poisson distribution by the method of percentiles, the method of probability weighted moments, the method of least squares, the method of weighted least squares, the method of generalized moments, and other methods. Another future work is to propose bivariate and multivariate generalizations of the linear failure rate Poisson distribution.

Appendix: Three data sets

The first data is

```
0.1102 0.2390 0.4598 0.7146 0.2608 0.0838 0.8746 0.1578
0.3358 0.0198 0.7192 0.7916 0.4486 0.4080 0.6048 0.3686
0.4686 0.5418 0.3760 0.8684 0.1572 0.4860 0.0118 0.4732
0.5450 0.8982 0.5674 0.2602 0.4330 0.3608 0.3648 0.5124
0.1360 0.7548 0.8960 0.4816 0.0818 0.3268 0.9514 0.8650
0.3372 0.5438 0.5392 0.5750 0.3672 0.6694 0.3068 0.2536
0.3756 0.3962 0.4690 0.3416 0.6430 0.9104 0.4426 0.7280
0.7370 0.7666 0.6420 0.2000 0.3588 0.6632 0.8752 0.8934
0.6526 0.1370 0.5222 0.7746 0.9230 0.6422 0.3298 0.7286
0.0054 0.3754 0.2448 0.9466 0.3256 0.3726 0.0516 0.4496
0.7850 0.8670 0.0758 0.5174 0.7742 0.5464 0.6152 0.7594
0.8310 0.4036 0.8954 0.7970 0.3638 0.0142 0.7998 0.1658
0.4572 0.7540 0.9220 0.3688
```

For computational stability with fitting distributions, we have divided each observation by 5000.

The second data is

```
1.293458333 0.251375000 1.265458333 1.404000000
1.280416667 1.201500000 1.193458333 0.340333333
1.101166667 1.059250000 1.360541667 1.245125000
1.098041667 1.049875000 1.167875000 1.271500000
1.182000000 0.925916667 0.963333333 1.119666667
0.867791667 0.845375000 0.803416667 0.323500000
1.165083333 1.065958333 1.103583333 1.035583333
1.173958333 0.886916667 0.789958333 0.671791667
0.782666667 0.534125000 0.691000000 0.813750000
0.773416667 0.629291667 0.520291667 0.635000000
```

```
0.695041667 0.712625000 0.428000000 0.423208333
0.615541667 0.254416667 0.160791667 0.125083333
0.416791667 0.215416667 0.214958333 0.185375000
0.228458333 0.206958333 0.228833333 0.190083333
0.205000000 0.007458333 0.192750000 0.227666667
0.155916667 0.179791667 0.018625000 0.169458333
0.066416667 0.005333333 0.115416667 0.080375000
0.495833333 0.854916667 0.498750000 0.902875000
0.967958333 0.786916667 0.920583333 0.943875000
0.807666667 0.761708333 0.733583333 1.043833333
0.893583333 0.746500000 0.736583333 0.880500000
0.889708333 0.780666667 0.668041667 0.861291667
0.711916667 0.718500000 0.863041667 0.908000000
0.833791667 0.671416667 0.826083333 0.823000000
0.784375000 0.667833333 0.669750000 0.835750000
```

For computational stability with fitting distributions, we have divided each observation by 1000.

The third data is

```
0.222673061 0.257639905 0.328155859 0.515672484
0.583401130 0.642256077 0.621521735 0.587506929
0.594755485 0.316753044 0.550884304 0.312962380
0.516646945 0.546445582 0.600493703 0.297813235
0.332441913 0.333245894 0.364800151 0.429097225
0.627439232 0.313363071 0.579554283 0.391397547
0.125167305 0.541816854 0.665764686 0.398880874
0.402492151 0.423982077 0.428143776 0.341767913
0.514537781 0.686683383 0.333088363 0.249962985
0.226748439 0.286643595 0.645490088 0.584664074
0.397377064 0.609634794 0.353187577 0.536304985
0.406031202 0.586163204 0.648786836 0.516497130
0.318475607 0.494774308 0.436782434 0.245923132
0.618409876 0.255245760 0.464312202 0.454133994
0.387982016 0.218311879 0.526363495 0.418258490
0.272839591 0.151997829 0.492728139 0.290973052
0.471553883 0.363069573 0.668371780 0.501805967
0.600306622 0.477109810 0.515188714 0.283784543
0.600625759 0.299420135 0.368553098 0.653382502
0.687845701 0.379423961 0.279504337 0.407995757
0.685695223 0.259685231 0.514854899 0.501119729
0.003522425 0.672089253 0.630145059 0.310811342
0.384073475 0.388312955 0.268080935 0.437408445
0.634243302 0.239656858 0.391844012 0.347107733
0.499160234 0.325770026 0.290634387 0.371908794
```

For computational stability with fitting distributions, we have divided each observation by 100.

Acknowledgments

References

Bain, L.J. (1974). Analysis for the linear failure rate life testing distribution. *Technometrics*, 16, 551–559.

Barreto-Souza, W., de Morais, A.L. and Cordeiro, G.M. (2011). The Weibull-geometric distribution. *Journal of Statistical Computation and Simulation*, 81, 645–657.

Ciumara, R. and Preda, V. (2009). The Weibull-logarithmic distribution in lifetime analysis and its properties, In *Proceedings of the XIIIth International Conference "Applied Stochastic Models and Data Analysis" (ASMDA-2009)*, editors L. Sakalauskas, C. Skiadas, and E.K. Zavadskas, Institute of Mathematics and Information/Vilnius Gediminas Technical University, Vilnius, Lithuania, 395–399.

Cox, D.R. and Hinkley, D.V. (1979). *Theoretical Statistics*. London: Chapman and Hall.

Dispenzieri, A., Katzmann, J., Kyle, R., Larson, D., Therneau, T., Colby, C., Clark, R., Mead, G., Kumar, S., Melton III, L.J. and Rajkumar, S.V. (2012). Use of monclonal serum immunoglobulin free light chains to predict overall survival in the general population. *Mayo Clinic Proceedings*, 87, 512–523.

Donida, G. and Mentrasti, L. (1982). A linear failure criterion for concrete under multiaxial states of stress. *International Journal of Fracture*, 19, 53–66.

Elhai, J.D. Calhoun, P.S. and Ford, J.D. (2008). Statistical procedures for analyzing mental health services data. *Psychiatry Research*, 160, 129–136.

Ferguson, T.S. (1996). *A Course in Large Sample Theory*. London: Chapman and Hall.

Ginebra, J. and Puig, X. (2010). On the measure and the estimation of evenness and diversity. *Computational Statistics and Data Analysis*, 54, 2187–2201.

Hong, Y. and Meeker, W.Q. (2013). Field-failure predictions based on failure-time data with dynamic covariate information. *Technometrics*, 55, 135–149.

Lehmann, L.E. and Casella, G. (1998). *Theory of Point Estimation*, second edition. New York: Springer Verlag.

Lu, W. and Shi, D. (2012). A new compounding life distribution the Weibull-Poisson distribution. *Journal of Applied Statistics*, 39, 21–38.

Mahmoudi, E. and Jafari, A.A. (2012). Generalized exponential-power series distributions. *Computational Statistics and Data Analysis*, 56, 4047–4066.

Prudnikov, A.P., Brychkov, Y.A. and Marichev, O.I. (1986). *Integrals and Series*, volume 1. Amsterdam: Gordon and Breach Science Publishers.

R Development Core Team. (2014). *A Language and Environment for Statistical Computing: R Foundation for Statistical Computing*. Vienna, Austria.

Reddy, Y.S.N. and Reddy, J.N. (1992). Linear and non-linear failure analysis of composite laminates with transverse shear. *Composites Science and Technology*, 44, 227–255.

Silva, R.B. Barreto-Souza, W. and Cordeiro, G.M. (2010). A new distribution with decreasing, increasing and upside-down bathtub failure rate. *Computational Statistics and Data Analysis*, 54, 935–944.

Singh, H. and Misra, N. (1994). On redundancy allocations in systems. *Journal of Applied Probability*, 31, 1004–1014.

Sutar, S.S. and Naik-Nimbalkar, U.V. (2014). Accelerated failure time models for load sharing systems. *IEEE Transactions on Reliability*, 63, 706–714.

van der Heijden, P.G.M., Bustami, R., Cruyff, M.J.L., Engbersen, F.G. and van Houwelingen, H.C. (2003). Point and interval estimation of the population size using the truncated Poisson regression model. *Statistical Modelling*, 3, 305–322.

Xu, S. and Hu, Z. (2011). Mapping quantitative trait loci using the MCMC procedure in SAS. *Heredity*, 106, 357–369.